Journal of Thermal Analysis and Calorimetry, Vol. 81 (2005) 51–55

SOLID–LIQUID PHASE EQUILIBRIA OF BINARY SALT HYDRATE MIXTURES INVOLVING AMMONIUM ALUM

*Y. Marcus**, *A. Minevich and L. Ben-Dor*

Department of Inorganic and Analytical Chemistry, The Hebrew University, Jerusalem 91904, Israel

The solid-liquid phase diagrams of binary mixtures of ammonium alum with ammonium iron(III) alum, with aluminum nitrate nonahydrate and with ammonium nitrate and of aluminum sulfate hexadecahydrate with aluminum nitrate nonahydrate are presented. The alum rich branches of the former three-phase diagrams were fitted by the Ott equation. The specific enthalpy of fusion/freezing of some compositions of the former three mixtures was determined by differential drop calorimetry.

Keywords: *aluminum salts, differential drop calorimetry, phase diagrams, salts hydrates*

Introduction

Solid–liquid phase diagrams of binary mixtures of salt hydrates have so far been published in very few cases only. The complete diagrams over the entire composition range for several divalent metal nitrates were reported by Mokhosoev and Got'manova [1]. The phase diagram of magnesium chloride and bromide hexahydrates was published by Marcus *et al*. [2]. We have recently reported the complete phase diagrams for the hydrates of magnesium nitrate and acetate, magnesium and aluminum nitrates, ammonium alum and ammonium sulfate, and ammonium alum and aluminum sulfate [3]. Also recently, Zeng and Voigt [4] showed isothermal phase diagrams involving quasi-binaries (binary salt hydrate mixtures) involving lithium nitrate trihydrate with magnesium nitrate hexahydrate, calcium nitrate tetrahydrate, and lithium perchlorate trihydrate, for which some experimental data near ambient temperatures were available. No liquidus curves of these systems were shown, however. Of course, many publications have dealt with salt hydrates, including mixtures, in the presence of excess water, for example the report by Ibnlfassi *et al.* [5], but these are not really relevant to the present subject.

In the present paper we report the phase diagrams of binary mixtures of ammonium alum (AAl) with ammonium nitrate (AN), of ammonium alum with aluminum nitrate nonahydrate (AlN), of ammonium alum with ammonium iron(III) alum (AFA), and of aluminum sulfate hydrate (AlS) with aluminum nitrate nonahydrate.

The enthalpy of fusion of some of the salt hydrates and their mixtures was measured by differential drop calorimetry (DDC) [6], to explore their suitability as phase change heat storage materials (PCMs).

Experimental

Materials

AAl: ammonium alum (Baker's Analyzed) $NH_4Al(SO_4)_2{\cdot}12H_2O$ was ground to smaller crystals before being melted. Its water content was determined by EDTA (back) titration of the aluminum content and was found to be 12.10±0.03 moles per mole salt. AlN: aluminum nitrate nonahydrate (Riedel-DeHaen) $Al(NO_3)_3{\cdot}9H_2O$ was used as received. Its water content was determined by EDTA (back) titration of the aluminum content and was found to be slightly below 9 moles per mole aluminum. A sample from a new bottle (Fluka) showed slightly more than 9 moles of water per mole salt, determined by weighing after drying in a vacuum oven at 60°C and 9.18±0.02 moles of water per mole salt, determined by EDTA (back) titration. FeN: iron(III) nitrate nonahydrate $Fe(NO_3)_3{\cdot}9H_2O$ (Fluka), was used as received only for the DDC measurements. AlS: two batches of aluminum sulfate (Baker's Analyzed) were used: one was nominally $Al_2(SO_4)_3{\cdot}18H_2O$ and the other $Al_2(SO_4)_3{\cdot}16H_2O$, but they actually contained 16.3±0.2 moles water per mole salt, from the water loss on heating to constant mass. They were used as received. AFA: ammonium iron(III) alum $NH_4Fe(SO_4)_2{\cdot}12H_2O$ (Merck), was the best available analytical reagent and was used as received. AN: ammonium nitrate NH_4NO_3 (AnalaR) was used as received. Ka: well crystallized kaolinite

* Author for correspondence: ymarcus@vms.huji.ac.il

1388–6150/$20.00

Akadémiai Kiadó, Budapest, Hungary
Springer, Dordrecht, The Netherlands

$Al_4Si_4O_{10}(OH)_8$ from Washington County, GA, and At, attapulgit (palygorskite) $(Mg,Al)_2Si_4O_{10}\cdot 4H_2O$ from Quincy, Florida, were used as nucleating and thickening agents.

X-ray characterization

A Philips Automatic Powder Diffractometer was employed, with monochromatized CuK_α radiation. Crystals of $Al(NO_3)_3\cdot 9H_2O$ (AlN), of $NH_4Al(SO_4)_2\cdot 12H_2O$ (AAl), and of $Al_2(SO_4)_3\cdot 16.3H_2O$ (AlS) were ground finely, and their powder diffractions were measured. The diffraction patterns agreed with those in the literature (2000 JCPDS, in the case of AlS with that of nominally $Al_2(SO_4)_3\cdot 17H_2O$) [7]). The possibility of a reaction of molten ammonium alum with kaolinite (Ka), used as the nucleation agent, has already been disproved previously [3] by X-ray diffraction.

Cooling curves and phase diagrams

Around 20 g total of the two salts were mixed on a mole fraction basis, ground together slightly, and 1% by mass of Ka or At was optionally added. The mixtures were heated in open test-tubes to 5–10 degrees above their melting points, and cooled in air with manual stirring till solidification. Cooling curves of the molten samples were taken as previously described with automatic recording of the temperatures [3]. Three cycles of melting and solidification were generally run, with concordant results within ±1°C of the temperature halt signifying freezing that was verified visually.

Differential drop calorimetry (DDC)

This technique was described in detail previously [6]. It was applied with 3.00 g samples dropped into the calorimeter and 40.0 g dodecane in the calorimeter as the calorimetric fluid. Samples of melts were dropped into the calorimeter at several temperatures T above the melting point, t_m, and samples of crystals were dropped at several temperatures T below t_m. The temperature rises, ΔT, at the inflexion points of the calorimetric curves were recorded. The difference, $\Delta\Delta T$, between the straight lines obtained from plotting the $\Delta T(T)$ values for the melts and crystals, extrapolated to t_m, was obtained. It was multiplied by the heat capacity of the system, $C_{p\,syst}$, calibrated electrically and with acetamide [6], to yield the total heat, Q, supplied to the calorimeter by the process of sample freezing. This quantity, divided by the mass of sample employed, finally gives the specific enthalpy of freezing, $\Delta_f H$/J g^{-1}. These determinations are expected to have a probable error of ±4 J g^{-1}.

Results

Ammonium alum (AAl) and ammonium iron(III) alum (AFA) mixtures

Neat AFA, the crystals of which are pale violet, melts at 30.5±0.5°C to a brownish yellow liquid. To obtain clear melts 1 drop concentrated sulfuric acid was added per 1.5 g AFA, neat or in a mixture. Considerable supercooling is noted for neat AFA and melts are stable at room temperature for long periods of time. Neat AAl melts at 90±1.0°C [3]. The mixtures were heated to 5–10 degrees above their melting points, producing melts of the same brownish yellow color, and cooled in air. Supercooling of 2–4 degrees was generally found before the halt in the temperature decrease, t_m, signifying crystallization, was noted. The phase diagram is shown in Fig. 1. A small dip in the otherwise monotonous decrease of t_m with increasing x_{AFA} is noted at x_{AFA}=0.4 and has been reproduced in three melting/freezing cycles.

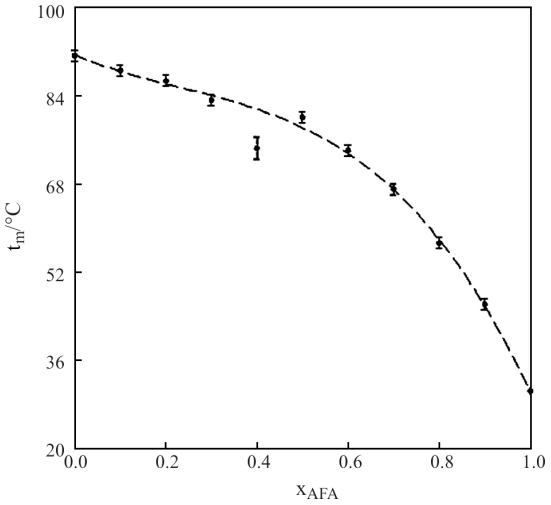

Fig. 1 The phase diagram of ammonium alum (AAl) with ammonium iron(III) alum (AFA). The dashed line is modeled according to Eq. (1)

Ammonium alum (AAl) and aluminum nitrate (AlN) mixtures

Neat AlN melts at 71.0±0.7°C [3]. In the mixtures, supercooling of 2–4 degrees was generally found before the halt in the temperature decrease, t_m, signifying crystallization. The phase diagram is shown in Fig. 2. A small dip in the decrease of t_m with increasing AlN content at x_{AlN}=0.60 and a definite maximum at x_{AlN}=0.70 are noted as well as a deep minimum at x_{AlN}=0.90. The solidified melts with the compositions x_{AlN}=0.50 and 0.70 were ground finely and their powder diffraction pattern were obtained. They showed the lines corresponding to the two components with no definite indication of the formation of a new com-

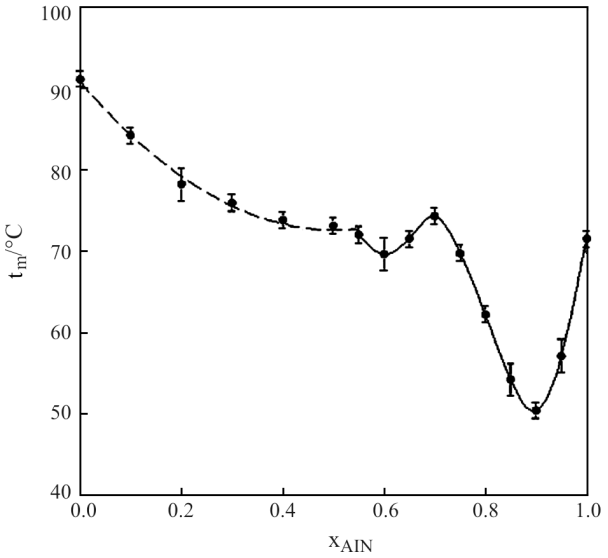

Fig. 2 Phase diagram of ammonium alum (AAl) with aluminum nitrate nonahydrate (AlN). The dashed line is modeled according to Eq. (1), the continuous line connects the data points

pound. From a concentrated aqueous solution of these salts only the alum crystallized.

Ammonium alum (AAl) and ammonium nitrate (AN) mixtures

The mixture containing 50% by mass of AN (85 mole%) was said [8] to be the eutectic, but no phase diagram supporting this was shown. We therefore obtained the full phase diagram of this system up to 95 mole% of AN, as shown in Fig. 3. (Neat AN melts and sublimes at considerably higher temperatures.) Considerable undercooling was observed, even with 1% Ka. Over a wide concentration range a second halt in the cooling curves was observed, signifying eutectic formation, although its reproducibility was not very good. The small unevenness in the t_m *vs.* x_{AN} curve up to x_{AN}=0.5 is probably not significant.

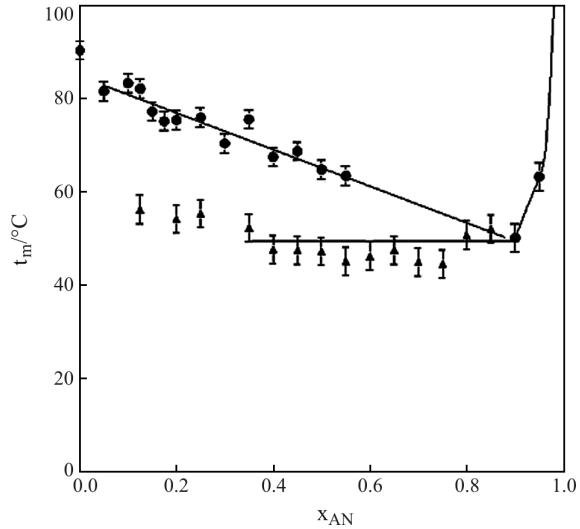

Fig. 3 Phase diagram of ammonium alum (AAl) with ammonium nitrate (AN). Circles pertain to the first break in the cooling curve and triangles to the second break, signifying the melting point of the eutectic, shown by the short-dashed horizontal line. The long-dashed line is modeled according to Eq. (1)

Aluminum sulfate (AlS) and aluminum nitrate (AlN) mixtures

Neat AlS melts at 93±1.0°C [3]. Undercooling in this system was not large so that the addition of Ka was immaterial and the results for three cycles agreed well. The resulting phase diagram is shown in Fig. 4. A sharp minimum is observed at x_{AlN}=0.90 with t_m=55.5±1.0°C. However, no second halt, signifying the eutectic, was observed at lower x_{AlN}. A second feature, that could possibly be a congruently melting material was observed at x_{AlN}=0.5±0.1, with t_m=79±1°C. This subject was not pursued further.

Differential drop calorimetry (DDC)

The molar enthalpies of fusion measured by this technique [6] are shown in Table 1 and compared there with values from the literature where available. DDC was applied to two mixtures of AAl and AFA at x_{AFA}=0.3 and 0.5, to three mixtures of AAl and AlN at x_{AlN}=0.25, 0.50, and 0.75 and to four mixtures of AAl and AN at x_{AN}=0.30**,** 0.40, 0.60 and 0.85 with results shown in Table 1. DDC was also applied to pure FeN with results shown in this Table, to be used in a subsequent study.

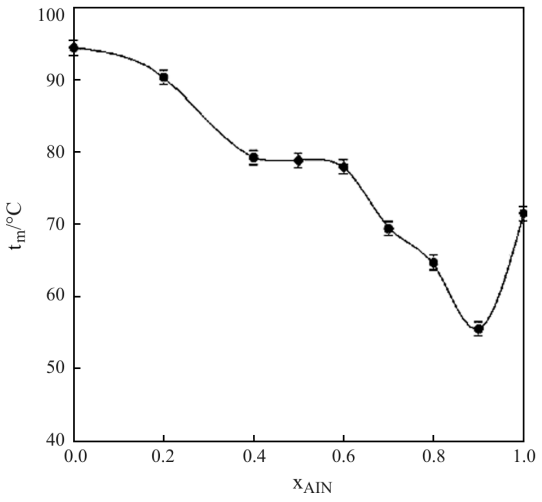

Fig. 4 Phase diagram of aluminum sulfate hydrate (AlS) with aluminum nitrate nonahydrate (AlN). The continuous line was drawn to pass through the experimental points

Table 1 Heats of fusion of AAl + AFA, AAl + AlN, and AAl + AN mixtures obtained by DDC

Salt composition	t_m/°C	ΔT/K	$C_{p\,syst}$/ J K^{-1}	Q/J	$\Delta_f H$/J g^{-1}
AAl	90		150		212[a], 228[b]
70AAl+30AFA	84	2.97	150	446	148
50AAl+50AFA	80	1.38	150	207	69
75AAl+25AlN	78	2.70	145	391	131
50AAl+50AlN	74	2.00	155	310	103
30AAl+70AlN	75	1.45	140	210	70
AlN	71	3.12	156	487	162, 176[b]
FeN	43	2.63	145	381	127
70AAl+30AN	82	3.14	145	455	152
60AAl+40AN	47	3.76	145	545	181
40AAl+60AN	55	3.10	145	450	150
15AAl+85AN	52	3.30	154	508	169, 170[c]

a – Mean value from [6], b – Values from [9], c – Value from [8]

Discussion

As mentioned previously [3, 9] the fusion/freezing points t_m of the salt hydrates reported in the literature vary considerably, depending on the method of determination (initial or complete melting or initial or final crystallization, as observed, e.g., in DSC) and on the exact water contents of the samples. The values obtained in the present work for the neat salt hydrates agree with those reported by us previously and with the better characterized literature values.

Binary A+B sytems with a single eutectic can be modeled by the Ott [10] expression:

$$t_m = t_{m\,A}[1+\Sigma a_i(x_B - 1)^i] \quad (1)$$

for the A-rich branch, where *A* crystallizes, and similarly for the other one. For the AAl+AFA system, where *A*=AAl and *B*=AFA, the entire diagram can be modeled by Eq. (1) with the coefficients a_0=–0.666, a_1= –1.902, a_2= –2.187, and a_3= –0.952, as shown in Fig. 1. AAl and AFA have the same cubic crystalline structure, space group Pa3, with the latter having an only slightly larger unit cell length, 12.313 Å, than the former, 12.240 Å [11]. It is likely, therefore, that they produce solid solutions when crystallizing from the mixed melts. Mixed crystals, dilute in AFA, have indeed been obtained from aqueous solutions [12]. The dip below this curve at x_{AFA}=0.4, although reproduced in three melting/freezing cycles, could still be an artifact, since it is unlikely that a compound is formed at the equimolar composition with a higher melting point than the solid solutions at compositions on both sides of x_{AFA}=0.5. The heat evolved on freezing of the mixtures examined, Table 1, are considerably lower than for pure AAl, and in spite of the advantageous somewhat lower melting points are not encouraging the use of such mixtures for heat storage.

The phase diagram of AAl+AlN is more complicated. This is not strictly a common cation binary mixture, unless AAl dissociated completely in the melt to yield ammonium and aluminum cations. AlN crystals are monoclinic, space group $P2_1/c$ [13], and unlikely to form mixed crystals with AAl. The reproducible maximum in the diagram at $x_{AlN}\approx 0.7$, however, does not indicate according to the X-ray diffraction that a compound is formed, that then yields a deep eutectic with neat AlN. The AAl-rich part of the diagram can be modeled according to Eq. (1), with a_0=–0.0094, a_1=0.783, and a_2=0.989, as shown in Fig. 2. The heat evolved on freezing of the mixtures examined, Table 1, are considerably lower than for pure AAl**,** and in spite of the lower melting points are not encouraging the use of such mixtures for heat storage.

Ammonium nitrate, AN, melts at 170°C and has several solid-solid transitions below, and it sublimes with decomposition above, temperature [14, 15] that is outside the range of measurements carried out here. Hence, the phase diagram was measured only up to x_{AN}=0.95 rather than to neat AN. The reproducibility of the halt temperatures in the cooling curves was not as good as with the other systems studied, with up to 2°C differences between the results of the three cycles of fusion/freezing carried out. Still, the AAl-rich part of the diagram, where the alum crystallizes on cooling the melts, up to x_{AN}~0.6 can be described by a straight line, or in terms of Eq. (1) with the coefficients a_0= –0.578 and a_1= –0.561. This straight line extrapolates to the eutectic composition and temperature, as seen in Fig. 1. A second halt in the cooling curve, signifying co-crystallization of AN, was seen at

x_{AN}≥0.35, but at AN contents of x_{AN}>0.5 only a single halt was found, corresponding to this eutectic. This was the case up to and including x_{AN}=0.9. The reported crystallization temperature [8], t_m=48°C for the x_{AN}=0.85 mixture, was confirmed, but this composition is certainly not a sharp eutectic minimum of the fusion temperatures. A possibly lower temperature of ~45±2°C was found at x_{AN} of 0.70 to 0.75°C. It is not clear why a broad composition region rather than a sharp value was obtained for the eutectic. The heats of freezing obtained for the mixtures, Table 1, are quite encouraging the use of such mixtures as phase change materials (PCMs) for heat storage. In fact, the mixture with x_{AN}=0.85 has been shown to be stable over a large number of fusion/freezing cycles and absorb and deliver most of the heat thus stored [8, 16].

Finally, the phase diagram of AlS+AlN, Fig. 4, resembles that of AAl+AlN in that the former as the latter have a deep minimum at x_{AlN}≈0.90, but the former does not show a pronounced maximum but rather a plateau in the diagram at intermediate compositions. The data do not let themselves to be modeled according to Eq. (1).

The specific enthalpies of freezing, $\Delta_f H$, have been determined for the following salt hydrate mixtures: AAl+AFA, AAL+AlN, AAl+AN (this work) and MgN+AlN [3], as shown in Fig. 5. Except for the latter system the compositions have not been selected in sufficient detail in order to reach definite conclusions concerning the composition dependence, but general trends can be seen. For two of the systems, AAl+AFA and AAL+AlN, the $\Delta_f H$ values are lower for the mixtures than for the pure components. In the case of AAl+AFA this is consistent with the presumed formation of solid solutions, so that less enthalpy is released on crystallization. The maximum shown at an intermediate composition by the other two systems, AAl+AN and MgN+AlN, is not readily interpreted, since the phase diagrams do not indicate that a congruently melting compound is formed.

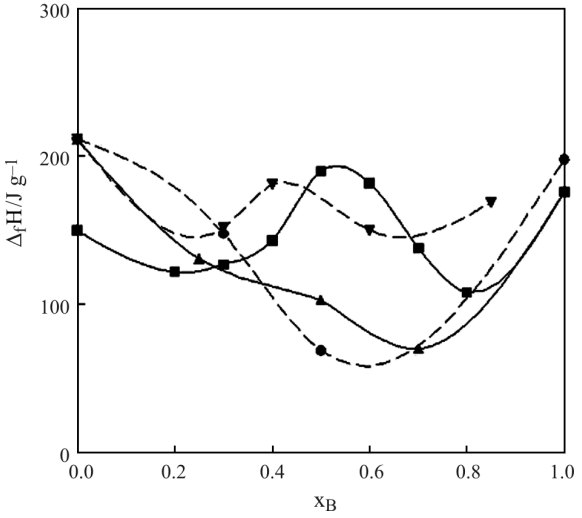

Fig. 5 The specific enthalpy of freezing of salt hydrate mixtures (A+B): ▲ – AAl+AFA, ▼ – AAl+AlN, ■ – AAl+AN, all from this work, and ● – MgN+AlN [3]

Acknowledgements

This research was supported by a grant from the Ministry of Science Culture Sport Israel and Forschungszentrum Juelich GmbH (KFA) within the German-Israeli Energy Research program. Ms. G. Wollmann is thanked for some of the X-ray diffraction measurements.

References

1 M. V. Mokhosoev and T. T. Got'manova, Russ. J. Inorg. Chem., 11 (1966) 466.
2 Y. Marcus, V. Dangor and S. Lessery, Thermochim. Acta, 77 (1984) 219.
3 Y. Marcus, A. Minevich and L. Ben-Dor, Thermochim. Acta, 412 (2004) 163.
4 D. Zeng and W. Voigt, Computer Coupling Phase Diagrams Thermochem., 27 (2003) 243.
5 A. Ibnlfassi, M. Kaddami and K. El Kacemi, J. Therm. Anal. Cal., 74 (2003) 341.
6 Y. Marcus, A. Minevich and L. Ben-Dor, J. Chem. Thermodyn., 35 (2003) 1009.
7 F. Cesbron and M. Sadrzadeh, Bull. Soc. Fr. Mineral Cryst., 96 (1973) 385.
8 C. K. Jotshi, C. K. Hsieh, D. Y. Goswami, J. F. Klausner and N. Srinivasan, Trans. ASME, 120 (1998) 20.
9 J. Guion, J. D. Sauzade and M. Laügt, Thermochim. Acta, 67 (1983) 167.
10 J. B. Ott and J. R. Goates, J. Chem. Thermodyn., 15 (1983) 267.
11 Natl. Bur. Stand. (US), Circ. 539, 6 (1956) 10, 539.
12 L. Campbell and S. Debenedetti, Phys. Lett., 20 (1966) 102.
13 Natl. Bur. Stand. (US), Circ. 25, 11 (1974) 6.
14 Ullmann's Encyclopedia of Industrial Chemistry, VCH, Weinheim, 1985, Vol.A2, p. 244.
15 W. A. Rosser, S. H. Inami and H. Wise, J. Phys. Chem., 67 (1963) 1753.
16 C. Vaccarino, G. Cimino, F. Frusteri and A. Barbaccia, Solar Energy, 34 (1985) 171.

Received: June 15, 2004
In revised form: December 14, 2004

DOI: 10.1007/s10973-005-6491-4